Fluorescent Probes

DOI: 10.1002/anie.200500845

In Vivo Optical Imaging of Amyloid Aggregates in Brain: Design of Fluorescent Markers**

*Evgueni E. Nesterov, Jesse Skoch, Bradley T. Hyman, William E. Klunk, Brian J. Bacskai, and Timothy M. Swager**

Neuroimaging is emerging as a way to noninvasively identify and monitor neurodegenerative diseases during the preclinical and early clinical stages.[1] Alzheimer's disease (AD) stands out among the neurodegenerative diseases as the fourth leading cause of death in the United States and the most common cause of acquired dementia.[2] Early detection of AD is imperative in enabling the understanding and clinical treatment of this disorder, as well as in preventing its progression. The characteristic signature of AD is the deposition of amyloid-β plaques and neurofibrillary tangles in the patient's brain,[3] which parallel the disease but can only be diagnosed with certainty after death by an autopsy.

A significant advance in the field has been the development of radiolabeled small-molecule agents capable of entering the brain and specifically targeting plaques and tangles for imaging with positron emission tomography (PET) and single-photon emission computerized tomography (SPECT).[1] A major limitation of these methods is the requirement for the markers to be labeled with short-lived isotopes, such as ^{11}C with a half-life of about 20 min for PET. An attractive noninvasive alternative is in vivo optical imaging using specific far-red (near-IR) fluorescent contrast agents. These contrast agents make use of the inverse fourth-power relationship between the wavelength and light scattering, thus allowing the longer-wavelength light penetration through the living tissues necessary for direct brain imaging.[4a] Long-wavelength detection methods also benefit from the low auto-fluorescence of biological matter beyond 600 nm.[4] The requirements for a successful optical marker of AD are: 1) a suitable wavelength interval of absorption and emission (600–800 nm), 2) the ability to rapidly enter the brain after intravenous injection, and 3) specific labeling of the amyloid-β deposits with rapid clearing of the unbound dye. Another unique advantage of optical imaging is the possibility to attain substantial differences in the photophysical/optical properties between the bound and unbound forms of the marker (requirement 4). This would allow a significant increase in imaging contrast which cannot be exploited with techniques based on radioligands.

Among the known amyloid-staining compounds, Congo Red (CR) provides historically the most standardized way of staining amyloid plaques, and is still employed in post mortem histological analysis of AD brain, as the binding is specific.[5] Thioflavin T (ThT) is another dye to use in analysis of aggregated amyloid proteins. It binds slightly weaker than CR, but makes up for this deficiency by exhibiting a green fluorescence, that becomes more than 1000 times brighter upon binding to amyloid plaques.[6] The understanding of what makes these simple molecules so specific to senile plaques is the starting point for the rational design of improved markers. Studies[7] suggest that the origin of the specific binding of CR to amyloid-β aggregates is due to the combination of electrostatic interactions between the negatively charged CR's sulfonate groups with the positively charged amino acid residues in the antiparallel protein

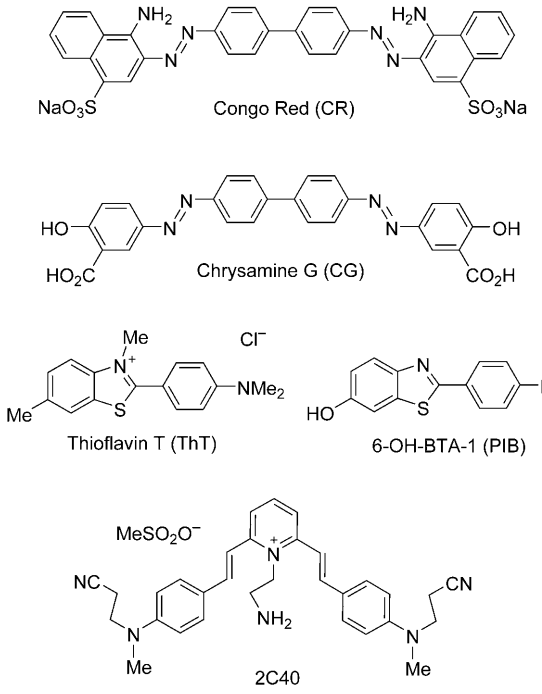

[*] Dr. E. E. Nesterov,[+] Prof. Dr. T. M. Swager
Department of Chemistry and
Institute for Soldier Nanotechnologies
Massachusetts Institute of Technology
Cambridge, MA 02139 (USA)
Fax: (+1) 617-324-0505
E-mail: tswager@mit.edu
J. Skoch, Prof. Dr. B. T. Hyman, Dr. B. J. Bacskai
Department of Neurology/Alzheimer's Disease
Research Laboratory
Massachusetts General Hospital
114 16th Street, Charlestown, MA 02129 (USA)
Prof. Dr. W. E. Klunk
Department of Psychiatry
University of Pittsburgh School of Medicine
Pittsburgh, PA 15213 (USA)
[+] Current address:
Department of Chemistry
Louisiana State University
Baton Rouge, LA 70803 (USA)

[**] This research was supported by NASA and the U.S. Army through the Institute for Soldier Nanotechnologies, under contract DAAD-19-02-D-0002 with the U.S. Army Research Office (TMS), by NIH through grant EB00768 (BJB).

Supporting information for this article is available on the WWW under http://www.angewandte.org or from the author.

β sheets, and CR's shape is complementary to features in an amyloid fibril's surface. The latter recognition likely involves hydrophobic interactions with the planarized aromatic π system of the dye molecule.[7c] Although the binding of ThT to amyloids has received less attention, it is likely to involve similar shape-specific recognition.[6,8] Thus, it is our opinion that the presence of hydrophobic planarized (or easily planarizable) π system is an important design feature to obtain high binding specificity.

A potential biomarker must be able to rapidly enter the brain after an intravenous injection. To exhibit high blood–brain barrier (BBB) permeability, the molecule needs to be relatively lipophilic (but not highly lipophilic as this will lead to its aggregation and accumulation in blood proteins and red blood cell membranes), and should not bear ionic groups. High BBB permeability also requires the marker to be relatively small, with an upper molecular weight limit of about 600 Da. These simple empirical rules are extremely robust, and, for example, both CR and ThT, as charged molecules, are not capable of crossing the BBB. It is also highly probable that any charged molecules like compound 2C40, a recently proposed fluorescent marker for AD found by combinatorial screening of a library of 320 compounds,[9] will be similarly incapable of in vivo imaging. In contrast, substantial increase of the BBB permeability was achieved with uncharged analogues of CR and ThT. For example, in the CR analogue Chrysamine G (CG), the replacement of the sulfonate group by a less ionizable carboxy group significantly increased the BBB permeability without compromising the high binding specifity.[10] A ThT uncharged analogue, 6-OH-BTA-1, which is commonly referred to as Pittsburgh compound B (PIB), is highly efficient both in crossing the BBB and in selective binding to AD amyloid aggregates, and is currently under clinical tests as an amyloid marker with PET imaging.[11]

To develop an effective in vivo imaging dye, we have merged these empirical requirements with electronic structure design to produce a compound possessing a suitable spectral range of the absorption and emission bands along with a potential to produce additional imaging contrast. We have employed a classical push–pull architecture with terminal donor and acceptor moieties that are interconnected by a highly polarizable bridge. Various donor and acceptor groups can be used to manipulate the relative energies of HOMO and LUMO, with better donor and better acceptor leading to a smaller HOMO–LUMO gap and to the desired long wavelength absorption/emission bands. Finally, to obtain greater imaging contrast, we required a molecule to possess a substantial degree of conformational freedom when unbound in solution, but it would be conformationally restricted upon binding to the protein. Such a "rigidification" decreases the vibrational-rotational processes that couple the excited and ground states, thereby decreasing the radiationless decay rate and increasing the fluorescence quantum yield of the protein-bound molecule.[12]

The proof-of-approach near-IR Alzheimer's dye NIAD-4[13] was designed to satisfy all four of the requirements above. This dye with a molecular weight of 334 Da is likely to be among the simplest possible structures. It uses a dithienylethenyl π-conjugated bridge between donor and acceptor. The highly polarizable bridge was chosen to provide a substantial bathochromic shift in both absorption and emission spectra of the dye. The rigid rodlike aromatic core of NIAD-4 is hydrophobic and readily planarizable, and has a shape similar to that of ThT for achieving a high binding specificity to amyloid aggregates. In unbound NIAD-4 free rotation around the single bonds leads to facile vibrationally coupled radiationless excited-state deactivation. Reduction of these processes upon binding to the protein aggregate was expected to enhance its fluorescence quantum yield. The donor and acceptor groups were chosen to balance between the need for a high electron-donating/accepting ability to achieve a substantial spectral bathochromic shift and the requirement to avoid charged or easily ionizable groups to improve the BBB permeability. The dicyanomethylene group was chosen as the acceptor, and the hydrophilic *p*-hydroxyphenyl group was selected as a donor to compensate for the high hydrophobicity of the bridge. Both groups are relatively small and were instrumental in maintaining the low molecular weight of NIAD-4.

The synthesis of NIAD-4 is shown in Scheme 1. The silyl-protected aldehyde **4** was prepared by Stille coupling.

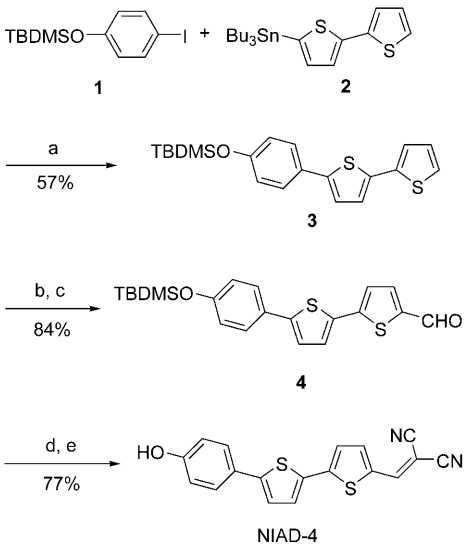

Scheme 1. Synthesis of dye NIAD-4: a) $[PdCl_2(PPh_3)_2]$ (3 mol%), toluene, 70°C, 36 h; b) *n*BuLi, TMEDA, hexanes, −70°C, 2 h; c) DMF, −70°C→RT, 12 h; d) $CH_2(CN)_2$, EtOH, piperidine (cat.), 60°C, 18 h; e) HCl, 60°C, 6 h. DMF: *N*,*N*-dimethylformamide; TMEDA: *N*,*N*,*N*′,*N*′-tetramethylethylenediamine.

Condensation with malononitrile followed by in situ deprotection afforded NIAD-4 as a dark-red material, which exhibits a bright red fluorescence in methanol solution (Figure 1). This contrast marker is slightly soluble in aqueous media, although it forms micelles/aggregates at the concentrations above 10 μM.[14] The aqueous solutions of NIAD-4 only have trace emission (quantum yield ≈0.00008), which may be in part due to the greater stabilization in aqueous media of the non-emissive intramolecular charge transfer state as opposed to the emissive planar excited state.[15] An in vitro spectral study with aggregated synthetic amyloid-β 1–

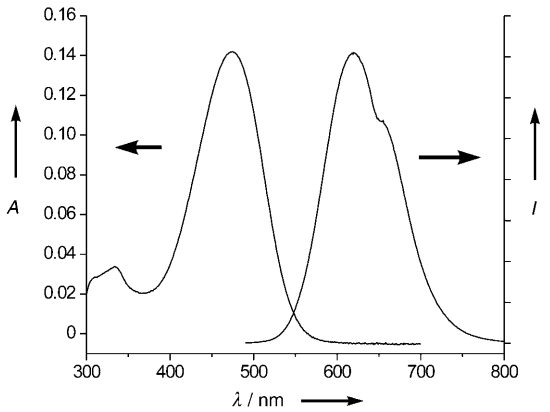

Figure 1. Absorption and fluorescence spectra of NIAD-4 in MeOH solution. (Extinction coefficient ε(475 nm) 35 700; fluorescence quantum yield 0.15.)

40 protein displayed a significant red shift ($\Delta\lambda \approx 70$ nm) of the absorption maximum along with about 1.3-fold increase in its extinction coefficient (Figure 2). This phenomenon is a

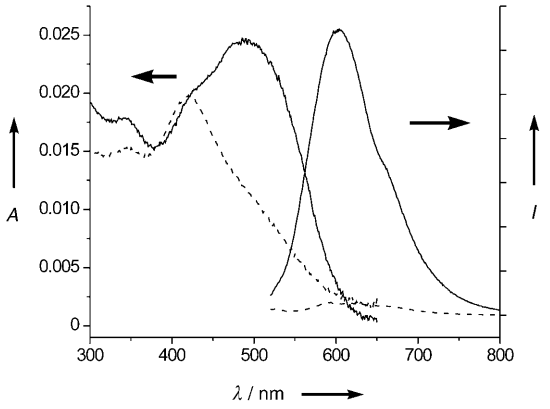

Figure 2. Absorption and fluorescence spectra of NIAD-4 in aqueous PBS solution in the presence of aggregated amyloid-β protein (solid line) and without the protein (dashed line). Concentrations: NIAD-4 4.1 μM, amyloid-β ≈10 μM. PBS: phosphate buffered saline.

consequence of the strong binding between the dye and the aggregated amyloid fibrils. The fluorescence maxima of the bound and unbound forms do not differ appreciably, and, as expected, the binding is accompanied by a dramatic enhancement of the fluorescent emission (about 400-fold, quantum yield 0.05), which is visible by simple visual inspection even at the micromolar concentrations used in the experiment. Apparently, the protein-bound dye is preorganized in a geometry that is similar to the planarized geometry of the emissive excited state after it has reached its equilibrium nuclear coordinates. Furthermore, binding to the amyloid fibrils places the dye in a lower dielectric constant environment that decreases detrimental relaxation into a non-emissive intramolecular charge transfer state.[15]

The binding studies with artificially aggregated amyloid protein assays revealed that NIAD-4 binds to the same site as BTA-1 with a binding affinity K_i of 10 nM. This affinity is much higher than that of ThT ($K_i = 580$ nM), and is close to that of high-affinity amyloid-binding compounds like PIB ($K_i = 4.3$ nM).[11b] The excellent performance of NIAD-4 for in vivo staining of amyloid plaques was demonstrated by using transgenic mice with AD-like pathology prepared with cranial windows to allow direct monitoring of the brain surface.[16] The dye readily crosses the BBB after an intravenous injection and labels specifically both the plaques and cerebrovascular amyloid angiopathy in the living brain thus making them easily detectable by the characteristic red fluorescence (see Figure 3 and Supporting Information). The high specificity of labeling the amyloid deposits is also clearly observed with in situ histochemical staining of fixed sections from transgenic mouse brain (Figure 3). In both in vivo and in situ experiments, the fluorescent images reveal exact position and size of the aggregated amyloid deposits, therefore providing the best demonstration of the high labeling specificity of NIAD-4.

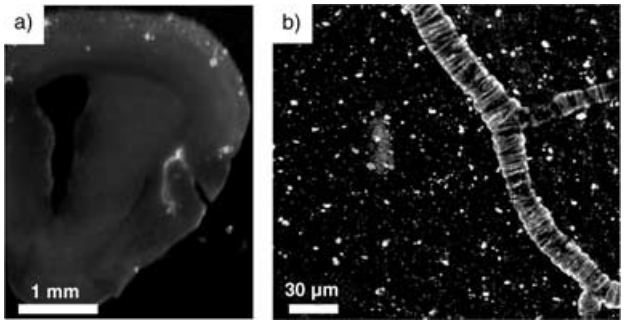

Figure 3. In vivo targeting and in situ specificity of NIAD-4 for amyloid deposits in the brain. a) A fluorescent image of a coronal section of brain from an aged APP transgenic mouse labeled with a 10 μM solution of NIAD-4 in DMSO/propylene glycol for 15 min at RT. b) In vivo fluorescent detection of both senile plaques and amyloid angiopathy using multiphoton microscopy immediately following intravenous injection of 2 mg kg^{-1} of NIAD-4. The images demonstrate the egress of dye through the BBB in a living mouse as well as the specific, sensitive targeting of amyloid-β deposits in the brain.

The remarkably strong bathochromic shift in absorption concomitant with the increase of absorption intensity upon binding combine for the high contrast optical imaging. To support our model that these changes are in part due to the planarization of NIAD-4 upon binding, we have calculated the geometry-optimized structure of the dye molecule (Figure 4a). Although both thienyl rings are nearly coplanar (dihedral angle 4.5°), the benzene ring is markedly twisted with respect to the plane of the neighboring thienyl group (dihedral angle 24.5°). This geometry still allows a π conjugation, and both HOMO and LUMO are substantially delocalized over the entire molecule (Figure 4c). Interestingly, just a small geometry change towards further planarization (which is likely to happen upon binding to amyloid fibrils) significantly increases the conjugation, resulting in even more delocalized frontier orbitals and a smaller HOMO–LUMO gap. The computed electrostatic potential distribution over the electron density surface (Figure 4b) is very similar to that of CR, with the highly hydrophobic neutral core and negative charge density localized at the

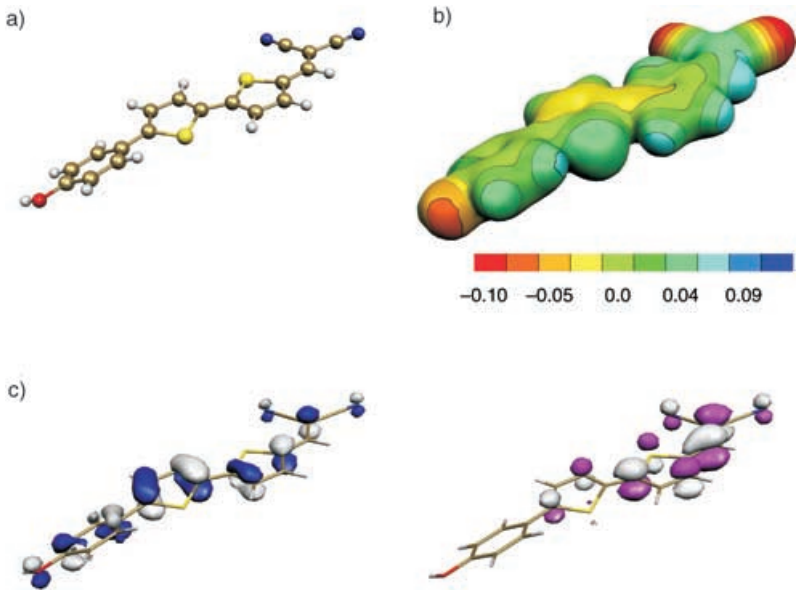

Figure 4. Optimized ground-state geometry of NIAD-4 (a), color-coded electrostatic potential mapped over electron density surface (b), and frontier molecular orbitals (c): HOMO (left) and LUMO (right). The computations were performed in gas phase at B3LYP/6-31G(df,p) level of theory. For this geometry, the computed absorption maximum (TD-B3LYP/6-31G(df,p)) was found to be 481 nm, which is in excellent agreement with the experimental value (475 nm).

molecule's termini. This feature may be in part responsible for the high binding selectivity of NIAD-4 to aggregated amyloid protein.[17]

In conclusion, we have demonstrated that the targeted rational design of in vivo fluorescent markers for amyloid protein aggregates can be successfully accomplished with a set of very simple qualitative rules. The designed contrast agent NIAD-4 shows remarkable promise for the optical imaging of amyloid plaques in brain. It may also be useful for the detection of peripheral amyloidoses. Clearly, its practical application in human Alzheimer's disease research and diagnostics requires further red-shifting of its spectral characteristics and increasing fluorescence quantum yield to allow truly noninvasive monitoring of the brain surface, without the need for the cranial window. It also requires detailed and thorough toxicity studies which we have not performed at this stage.[18] Still this is a remarkable milestone demonstrating great power of the simple design principles outlined herein for development of a practical AD biomarker. Regardless of the spectral properties of this new compound, a radiolabeled version of NIAD-4 may also be advantageous for PET or SPECT imaging. Directed modifications of the structure of NIAD-4 with the purpose to further red-shift the spectral characteristics, increase fluorescence quantum yields, and generally improve performance, as well as gain deeper understanding of these markers, are currently underway.

Received: March 7, 2005
Revised: July 16, 2005
Published online: August 1, 2005

Keywords: Alzheimer's disease · dyes/pigments · fluorescent probes · imaging agents · synthesis design

[1] S. T. DeKosky, K. Marek, *Science* **2003**, *302*, 830 – 834.
[2] "Alzheimer Disease": P. Nowotny, J. M. Kwon, A. M. Goate in *Encyclopedia of Life Sciences*, Macmillan Publishers, Nature Publishing Group, **2002**.
[3] P. M. Gorman, A. Chakrabartty, *Biopolymers* **2001**, *60*, 381 – 394.
[4] a) "Near-Infrared Dyes for High Technology Applications": E. Terpetschnig, O. S. Wolfbeis, *NATO ASI Ser. Ser. 3* **1998**, *52*, 161 – 182; b) A. Becker, C. Hessenius, K. Licha, B. Ebert, U. Sukowski, W. Semmler, B. Wiedenmann, C. Grötzinger, *Nat. Biotechnol.* **2001**, *19*, 327 – 331.
[5] G. T. Westermark, K. H. Johnson, P. Westermark, *Methods Enzymol.* **1999**, *309*, 3 – 25.
[6] E. S. Voropai, M. P. Samtsov, K. N. Kaplevskii, A. A. Maskevich, V. I. Stepuro, O. I. Povarova, I. M. Kuznetsova, K. K. Turoverov, A. L. Fink, V. N. Uverskii, *J. Appl. Spectrosc.* **2003**, *70*, 868 – 874.
[7] a) I. Roterman, M. Krol, M. Nowak, L. Konieczny, J. Rybarska, B. Stopa, B. Piekarska, G. Zemanek, *Med. Sci. Monit.* **2001**, *7*, 771 – 784; b) J. Sajid, A. Elhaddaoui, S. Turrell, *J. Mol. Struct.* **1997**, *408*/409, 181 – 184; c) R. Khurana, V. N. Uversky, L. Nielsen, A. L. Fink, *J. Biol. Chem.* **2001**, *276*, 22715 – 22721; d) D. B. Carter, K.-C. Chou, *Neurobiol. Aging* **1998**, *19*, 37 – 40; e) W. E. Klunk, J. W. Pettegrew, D. J. Abraham, *J. Histochem. Cytochem.* **1989**, *37*, 1273 – 1281.
[8] H. LeVine III, *Amyloid* **1995**, *2*, 1 – 6.
[9] Q. Li, J.-S. Lee, C. Ha, C. B. Park, G. Yang, W. B. Gan, Y.-T. Chang, *Angew. Chem.* **2004**, *116*, 6491 – 6495; *Angew. Chem. Int. Ed.* **2004**, *43*, 6331 – 6335.
[10] W. E. Klunk, M. L. Debnath, J. W. Pettegrew, *Neurobiol. Aging* **1995**, *16*, 541 – 548.
[11] a) W. E. Klunk, Y. Wang, G.-F. Huang, M. L. Debnath, D. P. Holt, C. A. Mattis, *Life Sci.* **2001**, *69*, 1471 – 1484; b) C. A. Mattis, Y. Wang, D. P. Holt, G.-F. Huang, M. L. Debnath, W. E. Klunk, *J. Med. Chem.* **2003**, *46*, 2740 – 2754; c) W. E. Klunk, H. Engler, A. Nordberg, Y. Wang, G. Blomqvist, D. P. Holt, M. Bergström, I. Savitcheva, G.-F. Huang, S. Estrada, B. Ausén, M. L. Debnath, J. Barletta, J. C. Price, J. Sandell, B. J. Lopresti, A. Wall, P. Koivisto, G. Antoni, C. A. Mathis, B. Långström, *Ann. Neurol.* **2004**, *55*, 306 – 319.
[12] The phenomenon of increasing the emission quantum yield in viscous solvents, where a conformationally labile molecule is vibrationally-restricted, is well documented for ThT (ref. [6]), as well as for some other fluorescent molecules (K. A. Willets, O. Ostroverkhova, M. He, R. J. Twieg, W. E. Moerner, *J. Am. Chem. Soc.* **2003**, *125*, 1174 – 1175).
[13] NIAD-4 is one of a series of contrast agents that we have been developing and testing. Additional NIAD compounds will be reported in the future.
[14] The 10 μM aggregation threshold, determined by a simple visual inspection, is a very approximate estimate, and strongly depends on the way the solution was prepared. The solutions used in the experiments reported herein had at least twice lower concentration, and their absorbance did not change after passing through a syringe filter with 0.2 μm pore size. Based on this, we can reasonably assume that NIAD-4 was not aggregated in the solutions.

[15] We are currently conducting computational studies to gain further insight into this phenomenon.
[16] B. J. Bacskai, G. A. Hickey, J. Skoch, S. T. Kajdasz, Y. Wang, G.-F. Huang, C. A. Mathis, W. E. Klunk, B. T. Hyman, *Proc. Natl. Acad. Sci. USA* **2003**, *100*, 12462 – 12467.
[17] Alternatively, the spectral changes upon binding to amyloid may be explained by change in protonation of the phenolic hydroxy group upon binding of the dye to a protein aggregate. This behavior should be similar to the deprotonation at higher pH values, which can be employed to study the deprotonation effect. Although these experiments showed an anticipated change in optical properties at increasing pH (Figure S1 in the Supporting Information), the overall trend does not correspond to the spectral changes found upon binding to amyloid. This allowed us to safely rule out the explanation based on the protonation change.
[18] Injection of NIAD-4 into living mice did not result in any substantial alteration of their normally expected lifespan, or showed any visually detectable abnormalities. Although this does not exclude the need for thorough toxicology experiments, it may indicate that the dye is not significantly toxic.

